

PROPERTIES OF THE TYPE 1A SUPERNOVA SN2013AA

EVAN AZEVEDO,¹ HENRY TAYLOR,¹ AND MARK WISCOMBE¹

¹ *University of California, Santa Barbara
Physics Department
Santa Barbara, CA 93106*

Abstract

Type 1a supernovae synthesize on the order of $1 M_{\odot}$ of radioactive Nickel, which powers its light curve. We present measurements of two important properties of the Type 1a supernova SN2013aa: distance to the object, and ^{56}Ni mass. We use images from the LCGOT telescope network, and analyze them by isolating for our object of interest, and plotting it's light curve. More specifically, we analyze astronomical images of the Type 1a supernova, SN2013aa, and determine the distance to the object, the mass of radioactive ^{56}Ni during peak emission, and the remaining ^{56}Ni mass after decay. By plotting the object's light curve we observe that our data spans the supernova's peak flux, as well as two stages of decay: $^{56}\text{Ni} \rightarrow ^{56}\text{Co}$ and $^{56}\text{Co} \rightarrow ^{56}\text{Fe}$. We use a commonly used value for the absolute magnitude of Type 1a supernovae $M_{abs} = -19.26 \pm 0.2$ to calculate the distance to the object $r = 24.53 \pm 0.27$ Mpc. By using M_{abs} again to calculate the nova's maximum bolometric luminosity, we find it's initial ^{56}Ni mass to be $M_{Ni} = 0.75 \pm 0.2 M_{\odot}$ at the peak of the event. Then, using this value we can fit linear models to the 2 decay stages we determine the remaining mass of Nickel after decay to be $M_{Ni,rem} = 0.0195 \pm 0.0053 M_{\odot}$. These findings agree well enough with accepted values of this event, but are observational in nature and unprofessional at best due to the lack of spectral data, data in the b band, and consistent data before the peak.

1. INTRODUCTION

Type 1a supernovae are bright astronomical events which are shown to occur in white dwarfs with Cobalt and Oxygen rich cores (Shen et al. 2010). Soon after collapse, the exploding star releases ejecta dominated by ^{56}Ni on the order of 1 M_\odot . The decay processes $^{56}\text{Ni} \rightarrow ^{56}\text{Co}$ dominates during the supernova's peak flux (Kasen 2014). The uniformity of the ejecta and absolute magnitude inherent to this event makes these events useful tools for approximation of distance to nearby objects. Due to these useful qualities, Type 1a supernovae are commonly used as “standard candles” for approximating distance to nearby objects of interest, determining the value of the Hubble constant, and other useful quantities (Branch and Miller 1993).

As stated above, Type 1a supernova synthesize on the order of 10^{-1} to 1 M_\odot of radioactive ^{56}Ni and have an absolute magnitude $M_{abs} \approx 19.5$. Knowing this allows us to determine the bolometric luminosity of our Type 1a supernova by assuming the energy of the photons produced by the ejecta, and the absolute brightness of the event. Then, by a calculation involving Arnett’s rule, we can determine the initial mass of ^{56}Ni , M_{Ni} , during the peak of the supernova. Again, the object’s light curve proves useful, as the slope of the curve after the peak indicates the decay rate of the supernova’s ^{56}Ni mass. The supernova also undergoes another branch of decay in the second part of the data, $^{56}\text{Co} \rightarrow ^{56}\text{Fe}$.

Lack of the full visible spectrum (b, g, and r) provides some hurdles for our group in creating a scientific image of the star field, and calculating apparent magnitude of the peak. We address these concerns by converting our g and r band data into the B band, and by averaging the decay rates of the three bands together. These methods provide us with reasonable estimations of real physical values of the Sn2013aa event.

2. METHOD

We begin with images taken by various telescopes in the LCGOT telescope network. Figure 1 shows scientific images of the star field of interest created with the image data given on two different days of observation. To graph our object’s light curve for analysis, we make catalog files of the stars and the magnitudes of their fluxes by running SExtractor and Match Stars programs edited for this purpose on the .fits files from observations of the star field. This gives us the locations, fluxes, and magnitudes of the matched stars in the captured star field, along with systematic error estimations. We then use code created in Python to take the Modified Julian Date (MJD), adjusted magnitude, and error in magnitude for matched stars in the (X,Y) location we identified in DS9 to be SN2013aa to isolate for the event of interest. This allows us to directly plot the light curve of SN2013aa in the 3 bands provided (Fig. 3).

In order to estimate the apparent magnitude at the peak in the visual spectrum, we transfer our g and r band data to the B band, using the relation $B = g + 0.51 + 0.60 * (g - r)$, found on the website <https://www.astro.umd.edu/ssm/ASTR620/mags.html>.

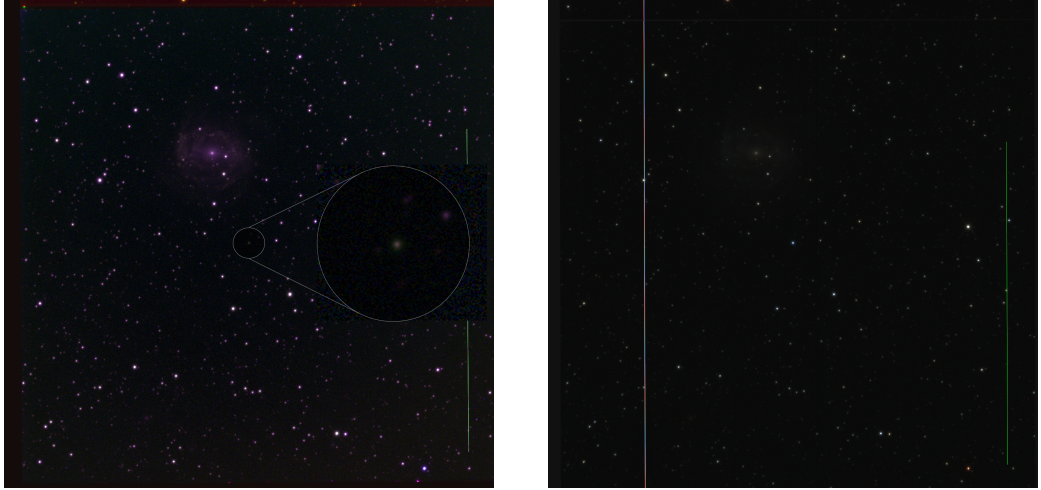


Figure 1. Left: Our scientific image of the star field, taken 3 months after its peak, created using STIFF on the g, r, and i bands. The object of interest, SN2013aa is circled and zoomed in the image to show its location and color. Notice that the object is more blue than other objects in this image.

Right: A scientific image of the star field during the supernova peak. We see that the event is much brighter than the nearby stars.

We then get a conversion factor for magnitudes from the files created by SExtractor. We find a nearby bright star TYC 7818-1437-1 and look it up on the Simbad database and use its B band magnitude to calculate a flat magnitude adjustment factor. We use this B band magnitude value on the peak day of the light curve to calculate the distance to SN2013aa with the relation:

$$r = 10^{\frac{M_B - M_{abs} + 5}{5}}, \quad (1)$$

where M_B = relative magnitude of the peak ejection in the B band, and $M_{abs} = 19.26 \pm 0.2$ is the cited absolute magnitude for type 1a supernovae (Richardson et al. 2014).

Next, we calculate the object's peak bolometric luminosity to calculate its radioactive Nickel mass. To do so, we use the standard equation relating magnitudes and luminosity:

$$M_{bol,*} - M_{bol,\odot} = -2.5 \log_{10} \left(\frac{L_*}{L_\odot} \right), \quad (2)$$

and approximate $M_{bol,*} \approx M_{abs}$. We use $M_{bol,\odot} = 4.74$, and $L_{bol,\odot} = 3.828 * 10^{33}$ ergs/s as reasonable, commonly accepted values for the Sun.

We then use an equation of Arnett's rule to calculate the ^{56}Ni mass, M_{Ni} (Childress et al. 2015).

$$\frac{M_{Ni}}{M_\odot} = \frac{L_{bol,*}}{(2 * 10^{43} \pm 0.3 * 10^{43}) \text{ergs/s}}. \quad (3)$$

Once we have the peak ^{56}Ni mass of the object, we fit linear regression to each of the 3 bands comprising our data to get the rates of ^{56}Ni decay (Figure 2). We started regression on the peak day, and ended at the last day before the gap in data for the

$^{56}\text{Ni} \rightarrow ^{56}\text{Co}$ decay. Similarly, we fit the 2nd part of the data after the gap for the $^{56}\text{Co} \rightarrow ^{56}\text{Fe}$ decay. we average the slopes in each band for both decay branches to arrive at the combined slope for both decays.

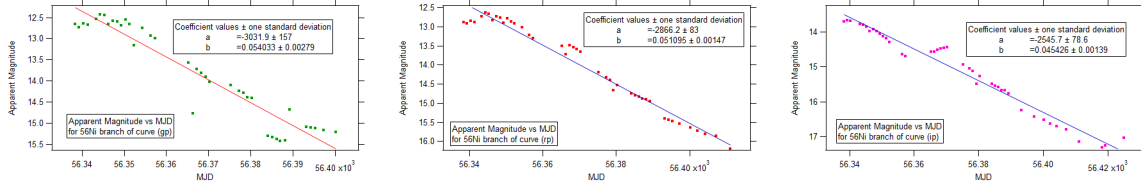


Figure 2. Fits of the $^{56}\text{Ni} \rightarrow ^{56}\text{Co}$ decay rates in each band. Notice that each adheres to a linear fit very well, yet they differ from each other in slope. Also notice a slight bump in the r and i bands after the peak. This is to be expected of Type 1a supernovae, but is not quite prominent in our data.

With the decay rates in hand, we simply use the standard decay equation:

$$\frac{N}{N_0} = e^{-\lambda t} \quad (4)$$

to determine the resultant ^{56}Ni mass after decay, N . In this equation, the slope of the Nickel decay is λ , and the initial mass $M_{Ni} = N_0$.

We run STIFF on our data in all 3 bands on the date 06/25/13 to create a scientific image of our star field, Figure 1. Instead of running for b, g, and r bands to create the image, we use g, r, and i, in that order. The result is a scientific image shifted to violet, but with a clear color difference between SN2013aa and the other objects in the image. We run STIFF again on data from the supernova's peak, giving the image to the right for comparison (Fig. 1).

3. RESULTS

Following our methods results in the following light curve (Fig. 3). Preliminary analysis reveals that there is a complete gap in our data in all three bands. Also of note is the increase in variance towards the second part of the data. Using the flat conversion factor and nearby star comparison method as discussed above, we obtain a peak magnitude in the B band $M_B = 12.6886$. The uncertainty in this number is the systematic uncertainty in the magnitude from the fits file of the peak day, added in quadrature with the error in B magnitude from Simbad.

Then, using the distance equation (1) gives us a result for the distance to SN2013aa, $r = 24.53 \pm 0.27$ Mpc. The uncertainty in this value is dominated by the uncertainty from M_{abs} , given by $M_{abs,\delta} = \pm 0.2$ Mpc. Then the final uncertainty ± 0.27 Mpc is $M_{abs,\delta}$ added in quadrature with the fractional error in B band magnitude. For reference, we can compare this value to the distance to its nearby galaxy, NGC 5643, which lies 16.9 Mpc away from Earth (NAS 2015). This gives us an error of 68.9% on the distance calculation from the expected value. Clearly, our uncertainty alone does not allow for this discrepancy, so we look towards other sources of error for this overestimation in the discussion section 4.

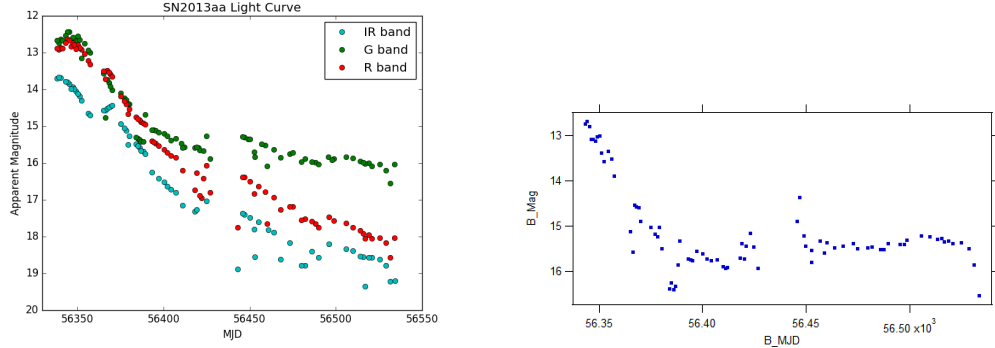


Figure 3. Left: Light curve of SN2013aa object in the g, r, and i bands. Right: Light curve in the B band. Both with flat scaling factors. Note: increase in variance in the 2nd stage of the collected data.

Using the magnitude luminosity relation (2), we calculate SN2013aa’s peak bolometric luminosity to be $L_{bol,*} = 1.5 * 10^{43} \pm 3.0 * 10^{42}$ ergs/s, giving a Nickel mass $M_{Ni} = 0.75 \pm 0.27 M_{\odot}$ from Arnett’s rule (3). The uncertainty in this value is found from the uncertainty in M_{abs} added in quadrature along with the fractional uncertainty in $L_{bol,*}$. This uncertainty is large, and is roughly equal to a third of the gross M_{Ni} . Fortunately, this value is well within the expected range of $M_{Ni} \approx 1 M_{\odot}$, but is also potentially down to half as much as this, based on our calculations.

Then the remaining ^{56}Ni from decay is found with Equation (4), and the averaged slopes for the two decay branches. We found the remaining mass to be $M_{Ni,rem} = 0.026 \pm 0.0055 M_{\odot}$ for the ^{56}Ni branch. This leaves us with $M_{Ni,rem} = 0.0195 \pm 0.0053 M_{\odot}$ after the ^{56}Co branch.

The scientific image we render is a violet shifted image of our star field (Fig. 1). The unbalance of color in the image is due to use of i instead of b when using STIFF to create the image. From Figure 3, we note that the i band is significantly lower than the other 2 bands in magnitude, especially towards the later data. This discrepancy likely is the cause of STIFF’s confusion in color mixing for this image, as the brightest layer is the g layer by far, and this is the layer occupying the I-B range in the software’s 3 band image creation. However, the spectra of the supernova is clearly different from the other objects in the image, making it identifiable from its bluish tint. By comparison, the image on the right of the supernova’s peak shows how bright the event is by how it overshadows the surrounding objects.

4. DISCUSSION

We first note that most of the days of data points are retained throughout the data processing, meaning that we lost only a small fraction of our data points during our analysis. Thus, we conclude that the gap in the light curve for SN2013 is a gap in observational fits in our data set, most likely from a break in observation in the LCGOT network of this star field.

Another noteworthy lack of data is in the lack of spectrographic data. With spectrographic data, we could calculate the bolometric luminosity by using a more rigorous method (Cano 2013), and thus the Nickel mass, more rigorously. This would be preferable to using $M_{bol,*} \approx M_{abs}$, or trying as we did to calculate bolometric flux, which we were not able to get with the flux in ADU from SExtractor.

On a similar note, my group and I experienced a lot of confusion about band conversions. Without a b band, we missed an important part of calculating B-V magnitudes, and resorted to using B magnitudes, which left out our i band data. This, I feel, was an important source of error in our distance calculation. With the i band in our max magnitude value, our overall magnitude would be greater, and the object would be closer both to Earth and to the accepted value in the distance calculation (1). Similarly, we apply the flat magnitude correction from Simbad before making the B magnitude conversion. This may be a mistake, because we have not converted to B band magnitudes before adding the offset, which is calculated from data in the B band.

Another method we used that could use improvement is the derivation of decay rate. Instead of averaging the rates of the 3 bands, it would be smarter to use a unified curve of the 3 bands for which we could fit a singular linear regression to. We attempted something similar with the B band magnitude curve (Fig. 3), but we saw worse results with this method. This was also the measurement ($M_{Ni,rem}$) that had the least information online, so we were unsure about how to check what a likely ^{56}Ni could be remaining after our observation dates.

While we retain most of the data points throughout the process as stated, some of the outliers in the light curve seem to be so far off from their peers that they could be different stars entirely. This would indicate imperfections in the processing of our images by SExtractor and Match Images, or in the object isolation part of our code. However, near the peak we see good behavior from all 3 bands, other than the distance from the i band to the other two. More likely, the flat scaling factor we added does not work as well for smaller magnitudes towards the end of the supernova, increasing the variance in the dates of the later data.

As stated above, this image is created from data on 6/25 of the year we observe the event, which is at least a full three months after the peak of the supernova (See section 2). One may expect that the object would be much dimmer well after the peak, and it is comparatively hard to see in this image, except that its color is different than the other objects in the image because of the source of its light curve. I'm comfortable that an expert in STIFF could use our data to the most and create a much nicer image with the three bands provided.

5. CONCLUSION

We plot SN2013aa's light curve through the peak of the event and during its decay process to determine some of its fundamental quantities. We then calculate the peak

apparent magnitude in the B band magnitude $M_B = 12.6886$, giving a distance measurement to SN2013aa of $r = 24.53 \pm 0.27$ Mpc, which is 69% larger than the accepted value. Using an adapted form of Arnett's model, we calculate the event's peak $M_{Ni} = 0.75 \pm 0.27$ M_\odot , a highly uncertain value which is slightly lower than other reported values of this event. By analyzing the object's light curve as containing two stages of decay, we calculate the final Nickel mass at the end of observation to be $M_{Ni,rem} = 0.0195 \pm 0.0053$ M_\odot , leaving us with a small fraction of the initial M_{Ni} from the event. Our results agree well enough with cited measurements of this event to know that we had the right direction with our methods, yet some conceptual gaps prevented us from getting truly good values.

Without b band data, our scientific image of the star field was highly color shifted. We believe that other groups could improve on the apparent magnitude calculation on the peak day by incorporating the i band. Incorporation of spectral data for this event, which appears to have been observed enough to find easily, would improve the M_{Ni} calculation by allowing for more sophisticated calculations of $L_{bol,*}$, such as the method in Cano's paper.

6. ACKNOWLEDGEMENTS

I would like to acknowledge my partners, Henry and Mark for their dedication and effort in putting this project together. I would also like to thank our TA, Sarah, for her insight and positivity in the lab environment, and Ben for this interesting project and well structured & engaging course.

REFERENCES

- K. J. Shen, D. Kasen, N. N. Weinberg, L. Bildsten, and E. Scannapieco. Thermonuclear .Ia Supernovae from Helium Shell Detonations: Explosion Models and Observables. *ApJ*, 715: 767–774, June 2010.
doi:10.1088/0004-637X/715/2/767.
- D. Kasen. The theoretical understanding of type 1a supernova lightcurves. Powerpoint presentation, 2014.
- D. Branch and D. L. Miller. Type IA supernovae as standard candles. *ApJL*, 405:L5–L8, March 1993.
doi:10.1086/186752.
- D. Richardson, R. L. Jenkins, III, J. Wright, and L. Maddox. Absolute-magnitude Distributions of Supernovae. *AJ*, 147:118, May 2014.
doi:10.1088/0004-6256/147/5/118.
- M. J. Childress, D. J. Hillier, I. Seitenzahl, M. Sullivan, K. Maguire, S. Taubenberger, R. Scalzo, A. Ruiter, N. Blagorodnova, Y. Camacho, J. Castillo, N. Elias-Rosa, M. Fraser, A. Gal-Yam, M. Graham, D. A. Howell, C. Inserra, S. W. Jha, S. Kumar, P. A. Mazzali, C. McCully, A. Morales-Garoffolo, V. Pandya, J. Polshaw, B. Schmidt, S. Smartt, K. W. Smith, J. Sollerman, J. Spyromilio, B. Tucker, S. Valenti, N. Walton, C. Wolf, O. Yaron, D. R. Young, F. Yuan, and B. Zhang. Measuring nickel masses in Type Ia supernovae using cobalt emission in nebular phase spectra. *MNRAS*, 454: 3816–3842, December 2015.
doi:10.1093/mnras/stv2173.

NASA/IPAC Extragalactic Database
results for ngc 5643. <http://ned.ipac.caltech.edu/cgi-bin/nph-objsearch?objname=NGC+5643>,
2015. Accessed: 2017-01-09.

Z. Cano. A new method for estimating
the bolometric properties of Ibc
supernovae. *MNRAS*, 434:1098–1116,
September 2013.
doi:10.1093/mnras/stt1048.